A novel path planning approach for smart cargo ships based on anisotropic fast marching

Xin-ping Yan[1, 2, 3], Shu-wu Wang[1, 2, 3], Feng Ma[2, 3*], Yuan-chang Liu[4], Jin Wang[5]

[1] School of Energy and Power Engineering, Wuhan University of Technology, Wuhan, People's Republic of China.

[2] Intelligent Transport System Research Center, Wuhan University of Technology, Wuhan, People's Republic of China.

[3] National Engineering Research Center of Water Transportation Safety (WTSC), Wuhan, People's Republic of China.

[4] Department of Mechanical Engineering, University College London, Torrington Place, London WC1E 7JE, UK.

[5] Liverpool Logistics, Offshore and Marine (LOOM) Research Institute, Liverpool John Moores University, Liverpool, UK.

* Corresponding author.

E-mail addresses: xpyan@whut.edu.cn (X. P. Yan), wangshuwu@whut.edu.cn (S. W. Wang), martin7wind@whut.edu.cn (F. Ma), yuanchang.liu@ucl.ac.uk (Y. C. Liu), J.Wang@ljmu.ac.uk (J. Wang).

Abstract: Path planning is an essential tool for smart cargo ships that navigate in coastal waters, inland waters or other crowded waters. These ships require expert and intelligent systems to plan safe paths in order to avoid collision with both static and dynamic obstacles. This research proposes a novel path planning approach based on the anisotropic fast marching (FM) method to specifically assist with safe operations in complex marine navigation environments. A repulsive force field is specially produced to describe the safe area distribution surrounding obstacles based on the knowledge of human. In addition, a joint potential field is created to evaluate the travel cost and a gradient descent method is used to search for appropriate paths from the start point to the end point. Meanwhile, the approach can be used to constantly optimize the paths with the help of the expert knowledge in collision avoidance. Particularly, the approach is validated and evaluated through simulations. The obtained results show that it is capable of providing a reasonable and smooth path in a crowded waters. Moreover, the ability of this approach exhibits a significant contribution to the development of expert and intelligent systems in autonomous collision avoidance.

Keywords: Path planning; Smart ships; Fast marching method; Anisotropic fast marching method; Navigation brain system (NBS).

1 Introduction

In recent decades, Unmanned Ground Vehicles (UGVs), Unmanned Aerial Vehicles (UAVs) and Unmanned Surface Vessels (USVs) have been well developed and researched. With the maturing of technologies, the rapid development of UGVs, UAVs and USVs has inspired many researchers to explore unmanned or smart cargo ships. In addition, the reshaping of the shipping industry also contributes to the development of smart cargo ships, especially with the aim of reducing crew costs and human errors. Such a drive can be further revealed from recent maritime market needs. First, the Baltic Dry Bulk Index (BDI), which is the economic indicator of the shipping industry, has been hovering at a low level for years. Shipping enterprises are required to reduce costs by cutting down crews. In the meantime, authoritative maritime accident investigations elaborate that about 80% of marine accidents are caused by human failures (Spahn, Dorp, & Merrick, 1998; Antão & Soares, 2008; Celik & Cebi, 2009; Chen, Yan, Huang, Yang, & Wang, 2018). Lastly, the energy saving and emission reduction of ships have become a realistic requirement of the shipping industry. According to a number of reports published by relevant authorities, it has been claimed that the success in developing and utilising autonomous navigation can effectively improve the operating efficiency of a cargo ship, and reduce carbon emissions (Rolls-Royce, 2016).

The intelligence in autonomous navigation of USVs, including path planning and obstacle avoidance has been comprehensively studied, which has promoted the wide application of USVs in many fields such as surveying and mapping, military investigation, search and rescue, and hydrogeological investigation. However, the intelligence of USVs is difficult to be applied in common cargo ships. This is because, in general, the USVs are small, fast and easy to be manoeuvred. For instance, it is always easy to make a sharp turn for collision avoidance for USVs even in a complex navigation environment. In contrast, ships, especially cargo ships, are usually larger, slower and more difficult to manoeuvre. Therefore, a collision is often inescapable when the obstacle is in a position that is too close for a cargo ship to make evasive actions. In order to achieve the autonomous navigation of a cargo ship, Yan *et al.* (2017) put forward an intelligent system, namely Navigation Brain System (NBS), which is composed of three subsystems: a perception module, a cognizing module and a decision and manipulation module. Particularly, path planning for obstacle avoidance is an integral part of this system. It should be noted that an appropriate path should always be planned in advance not only for static obstacles but for dynamic ones. This is because when avoiding a static obstacle, it becomes relevantly easy to retain a safe distance to obstacles, which is the principle of collision avoidance. However, when a ship is encountering with a dynamic obstacle, especially with another ship, different risk levels exist due to different encountering situations with such a dynamic obstacle. In general, a conservative distance is recommended in collision avoidance, and many traditional methods, including Artificial Potential Field (APF), A*, Rapidly-

exploring Random Tree (RRT) and RRT*, have been introduced in such an application, but none of them is able to fully satisfy the dynamic characteristics of a cargo ship and the navigational conventions. For example, by taking into account the modelling of the motion of a moving ship, APF generally describes the ship (dynamic obstacle) as a gradient eclipse, of which the major axis is consistent with the course of the corresponding ship (Ma, Chen, Huang, Yan, & Wang, 2016). However, the risk levels of the convergence situations with its bow and stern are different for another ship. Also, the local optima problem remains to be complicated and tricky in APF, which will cause the ship to fail to find any evasive route.

Hence, the motivation of this paper is to develop a reliable path planning approach for smart cargo ships in autonomous intelligence based on their manoeuvring characteristics and the human knowledge of the safe area surrounding obstacles. In this research, a novel anisotropic FM-based path planning approach is proposed. First, based on the anisotropic FM method, a potential field model of an oval shape is proposed to describe the motion of moving ships or other dynamic obstacles. With the help of such a shape, the speed and course, or the dynamic characteristics of the ship can be fully described. Then, the isotropic FM method is used to generate a consuming time field by taking into account the start point as a zero value. Subsequently, a satisfied, reasonable and smooth path can always be found by applying the gradient descent method. The prominent advantages of this approach include that a potential field model is specially designed for both static and dynamic obstacles, and the path generated is relatively safe and short. Moreover, the smooth path can be directly used in ship path tracking. The approach can work well on the condition that the exact information of the involved ships or obstacles including the position, course, size and shape can be obtained and the clearances between any two ships or obstacles on either side of the path are large enough for navigation. Otherwise, the reliability of the approach may decrease.

The presented approach is specially designed for safe navigation of cargo ships. At the beginning, the approach with different parameters can be integrated into an advisory system, which provides several paths for selection. Based on the operators' decisions, the parameters can be optimized gradually. Furthermore, the proposed approach with optimized parameters can be developed into an autonomous system, which automatically controls a ship together with an automatic pilot. The main contributions of this paper include the formulation of a novel potential field model to describe the safe area surrounding obstacles based on the knowledge of human and the development of a novel and feasible path planning approach for smart cargo ships to navigate in crowded waters. To sum up, the proposed path planning approach is based on the collision risk knowledge of human. Meanwhile, the approach can be used constantly optimize the path for navigation with the help of the expert knowledge. It is of great significance to promote the development of expert and intelligent systems in autonomous collision avoidance.

The rest of this paper is organised as follows. In Section 2, a variety of path planning methods are reviewed and analysed. Section 3 describes the fundamentals of the FM method and the details of an anisotropic FM-based path planning approach. The proposed approach is verified by simulations in Section 4. Section 5 concludes this paper and discusses future research.

2 Literature review

Path planning algorithms are one of critical aspects in robotic related research and have attracted substantial interests in its application in USVs. In the early stages, the evolutionary algorithm (EA) was frequently adopted to search for feasible navigation routes. Smierzchalski (1999) firstly employed the genetic algorithm to generate an appropriate route for a marine vessel and developed a solution for collision avoidance with moving ships by adopting ship domain areas. A similar approach was also used by Tam and Bucknall (2010), with a specific emphasis on the fact that the practical approach should comprise generating practical evasive manoeuvres adhering to International Regulations for Preventing Collisions at Sea (COLREGs). Tsou and Hsueh (2010) implemented an ant colony-based algorithm to design a decision-making system which can assist vessels in navigating in the maritime environment and also obey the COLREGs. However, the major drawbacks of the EA are the inconsistency and incompleteness of the searching result, which hinders its adoption for practical applications as the properties of the algorithm cannot be guaranteed (Tam & Bucknall, 2013; Kala, 2012).

The probabilistic path planning algorithm is also a commonly-used method, including Probabilistic Roadmaps (Kavraki, Svestka, Latombe, & Overmars, 1994) and RRT (Jaillet, Cortes, & Simeon, 2008; Hidalgo-Paniagua, Bandera, Ruiz-de-Quintanilla, & Bandera, 2018). The basic idea of probabilistic path planning is to randomly select non-collision candidate points in a space, then connect them to generate a path. Therefore, the reproducibility and repeatability of these algorithms cannot be guaranteed. In addition to this, the paths generated by these algorithms do not take safe distances to obstacles into consideration.

Hence, in recent years, to meet the needs of path planning, some other algorithms have also been applied, such as the grid-based and artificial potential field (APF) methods. Xue *et al*. (2011) improved the APF to provide a safe collision free path in congested environments where multiple vessels are required to avoid. Abu-Tair and Naeem (2012) designed a COLREGs compliant path planner by using a modified A* algorithm. A path trimmer is integrated into the A* algorithm to smooth the generated path, making it more feasible for the vehicle to follow. Tam and Bucknall (2013) proposed a cooperative path planning algorithm for USVs with the major objective of increasing the practicability and the completeness of the corresponding algorithm. In particular, improved consistency and completeness can be further achieved in a way that the same path can always be generated when the corresponding environment does not change. However, all of these studies consider the path planning problem from a conventional perspective, *i.e*. generating the path with the shortest distance while

avoiding obstacles. The performance of such methods does not fully satisfy the requirements of cargo ships, which needs to take the dynamic characteristics of ships into consideration.

Over the past few years, the FM method-based path planning algorithm has become a novel approach to generate smooth and persuasive paths for robots. The FM method searches for a path based on the potential field. However, different from the conventional way of combining all fields to generate the joint potential field, the FM method produces the potential field by simulating the propagation of an electromagnetic wave. Hence, the generated potential field has no local minima problems, which is the main drawback of the APF (Garrido, Moreno, & Blanco, 2008; Montiel, Orozco-Rosas, & Sepúlveda, 2015).

The FM method generates a path with the help of a gradient descent method over the joint potential field from the destination to the start point, and one of the most appealing features of the generated path is the guaranteed smoothness that the generated potential field does not have any discontinuity (Garrido, Moreno, & Lima, 2011). No further path smooth processing is required, since the path can be easily executed by a proper controller in practical applications (Alvarez, Gómez, Garrido, & Moreno, 2015). In the meantime, the FM method is generally with fast computation, which further promotes its utilisation in real-time navigation on practical platforms of autonomous underwater vehicles (Petres, Pailhas, Patron, Petillot, Evans, & Lane, 2008), unmanned aerial vehicles (Garrido, Malfaz, & Blanco, 2013) and USVs applications (Liu, Bucknall, & Zhang, 2017).

However, when facing the problem of collision avoidance on dynamic obstacles, the isotropic FM-based path planning approach uses the same method in the scenario of avoiding static obstacles. In this occasion, such a method does not take the type, velocity and direction of the dynamic obstacles into consideration. In fact, such factors are essential in the path planning when avoiding a collision. Hence, some researchers integrate the isotropic FM-based path planning approach with other models to deal with dynamic obstacles (Liu & Bucknall, 2015). However, this makes the approach complex and difficult to be applied.

In order to address the above problem, this research improves the isotropic FM-based path planning approach and proposes a novel path planning approach based upon anisotropic FM-based path planning approach. The main feature of the algorithm is that when planning a path in a complex navigation environment, the proposed approach is capable of optimising its coefficients by considering the characteristics of the corresponding obstacles and subsequently generating an appropriate and practical path for smart ships.

3 A proposed approach

This research proposes a novel path planning approach based on the anisotropic FM method. In order to elaborate the approach in detail, this section describes how it is applied for path planning. First, a problem of the minimum cost path is introduced and analysed. Continuous forms of the minimum cumulative with isotropic and anisotropic cost functions are provided subsequently. Then, in order to allow these cost functions to be solved in practice, the

functions are discretized and the corresponding numerical solutions are introduced in detail. Eventually, an anisotropic FM-based path planning approach is provided for smart ships to avoid obstacles in dynamic environments.

3.1 The minimum cost path problem

The minimum cost path problem is the priority in many fields including robotics, geometric optics, geographic information system and wire routing. Hence, it has been extensively researched for many years.

One form of the minimum cost path problem is to find the shortest path on a finite graph where every arc between any two adjacent vertices is assigned with a weight. The shortest path between the start point and the end point in the finite graph means the lowest cumulative cost among all legal paths. In graph theory literatures, many shortest path planning algorithms based on graph search and dynamic programming are proposed. The best-known one is proposed by Dijkstra (1959).

A more general form of the minimum cost path problem, which is put forward by Papadimitriou (Mitchell & Papadimitriou, 1991) and Mitchell (2000), is based on the propagation of light. The optimal path between two arbitrary points is found according to the well-known law of optics refraction. By comparison, this solution of minimum cost path problem is more suitable for smart ships, since it is always capable of generating smooth paths. Such a solution can be elaborated briefly as follows.

When facing the problem of path planning for smart ships, the cost function τ is defined by the Cartesian sampled data in 2D image space. The objective is to find a path $P(s):[0,\infty)\to R^2$ that minimizes the cumulative travel cost from a start point $\mathbf{x}_s$ to random end point $\mathbf{x}_e$ in R^2. If the cost τ is only a function of the location $\mathbf{x}$ in the image domain, the cost function is called isotropic. The minimum cumulative cost at $\mathbf{x}_e$ is defined as:

$$U(\mathbf{x}_e)=\min_{P_{\mathbf{x}_s\mathbf{x}_e}}\int_0^L \tau\left(P(s)\right)ds\,. \tag{1}$$

where *s* is the path length from start point to point $P(s)$. $P_{\mathbf{x}_s\mathbf{x}_e}$ is the set of all paths linking $\mathbf{x}_s$ and $\mathbf{x}_e$. The path distance is L and the start and end points are $\mathbf{x}_s=P(0)$ and $\mathbf{x}_e=P(L)$ respectively.

If the cost function τ is not only a function of the location $P(s)$ but also dependent on the local direction $P'(s)$ of travel, it can be called anisotropic in this occasion. The minimum cumulative cost is then defined as:

$$U(\mathbf{x}_e)=\min_{P_{\mathbf{x}_s\mathbf{x}_e}}\int_0^L \tau\left(P(s),P'(s)\right)ds\,. \tag{2}$$

Solving Eq. (2) is considerably more challenging than solving Eq. (1). In a continuous space, the solutions for the minimum cumulative cost are given by the Hamilton-Jacobi (HJ)

equation (Tsitsiklis, 1995) in principle. However, it is generally impossible to find a perfect solution for the HJ equation. In practice, numerical solutions are consistent with the viscosity solution, which is a compromised but feasible solution to the HJ equation (Crandall & Lions, 1983).

3.2 The isotropic fast marching (FM) method

It is very difficult to solve Eq. (1) directly. Usually, Eq. (1) will be transformed into another form (Cohen & Deschamps, 2001). During the researching process, some researchers found that the minimum cumulative cost *U*, also called the arrival time, satisfies the Eikonal equation as follows:

$$\|\nabla U\| = \tau . \tag{3}$$

In applications, the discrete version of Eq. (3) needs algorithms to reduce the computational cost. Hence, Rouy and Tourin (Rouy & Tourin, 1992) gave a discrete solution of Eq. (3) on a 2D Cartesian grid map (Fig. 1) as shown below, making a small step forward.

$$\max\left(u_C - u_{A+}, u_C - u_{A-}, 0\right)^2 + \max\left(u_C - u_{B+}, u_C - u_{B-}, 0\right)^2 = \tau_C^2 . \tag{4}$$

where the arrival time at point *A*+, *A*-, *B*+, *B*- and *C* are denoted as u_{A+}, u_{A-}, u_{B+}, u_{B-} and u_C respectively. τ_C is the cost function at point *C*.

Tsitsiklis (1995) and Adalsteinsson and Sethian (1995) proposed a solution independently to solve Eq. (4) by using a single-pass algorithm, which was named as “fast marching method” by Adalsteinsson and Sethian (1995). This algorithm calculates the value at every grid point in accordance with a strategy that is similar to the Dijkstra algorithm (Dijkstra, 1959). This strategy is based on the fact that the arrival time *U* at any point only depends on the neighbouring points. In fact, such neighbouring points generally have smaller values. Thus, it is only necessary to calculate the one sided differences when solving Eq. (4).

Taking the quadrant 1 as an example (Fig. 1), the solution of Eq. (4) is given by:

$$u_C = \begin{cases} \dfrac{1}{2}\left(u_{A+} + u_{B+} + \sqrt{2\tau_C^2 - \left(u_{A+} - u_{B+}\right)^2}\right) & \text{if } u_C > u_{A+} \text{ and } u_C > u_{B+} \\ \min\left(u_{A+}, u_{B+}\right) + \tau_C & \text{otherwise} \end{cases} \tag{5}$$

The same result can also be derived from the optimal trajectory problem rooted in the control theory as shown by Tsitsiklis (1995). In Fig. 1, it can be assumed that the minimal path starts from point *D* to point *C*. The arrival time at point *C* is denoted as u_C and calculated based on u_{A+} and u_{B+}. If the arrival time at point *D* is denoted as u_D, the arrival time u_C is the sum of u_D and the traveling time of wave from *D* to *C*. It can also be a reasonable hypothesis that the wave is planar. As a result, a linear interpolation can be used to find an approximated solution for u_D, defined as:

$$u_D = t u_{A+} + (1-t) u_{B+} . \tag{6}$$

In this occasion, the arrival time u_C can be given by the following equation:

$$u_C = \min_{t\in[0,1]}\left(tu_{A+} + (1-t)u_{B+} + \left\|\vec{\theta}\right\|\tau_C\right). \tag{7}$$

where t is given in Fig. 1, satisfying the conditions $0 < t < 1$. $\left\|\vec{\theta}\right\|$ is the length of vector CD and equal to $\sqrt{t^2 + (1-t)^2}$. The remaining three quadrants are handled in the same way and the arrival time value assigned to u_C is the smallest value of the four.

Eq. (7) can be solved either iteratively or analytically. The analytical solution can be deduced as below and it is exactly the same as Eq. (5).

$$\frac{du_C}{dt} = u_{A+} - u_{B+} + \frac{2t-1}{\sqrt{t^2 + (1-t)^2}}\tau_C = 0,$$

$$\Rightarrow t_{1,2} = \frac{1}{2} \pm \frac{u_{A+} - u_{B+}}{\sqrt{2\tau_C^2 - (u_{A+} - u_{B+})^2}},$$

$$\Rightarrow u_C = \frac{1}{2}\left(u_{A+} + u_{B+} + \sqrt{2\tau_C^2 - (u_{A+} - u_{B+})^2}\right).$$

The isotropic FM method uses Eq. (5) to update the minimum cumulative cost at each point. Compared with the Dijkstra algorithm (Dijkstra, 1959) the FM method is capable of providing a more smooth and continuous path. The isotropic FM method is summarized in Algorithm 1 and illustrated in Fig. 2. During the initialisation process, all the grid points are assigned with an infinity arrival time and grouped into three different categories, *i.e.* the *Far*, *Accepted* and *Trial* point sets. The operation is similar to the Dijkstra algorithm (Dijkstra, 1959). Each category is explained as follows:

- The *u*-values of points in the *Accepted* set will not be changed.
- The *u*-values of points in the *Trial* have been computed already but may be changed in future calculations.
- The *u*-values of points in the *Far* set have never been computed.

In each iteration when executing the algorithm, the point **x** with the smallest *u*-value will be taken out from the *Trial* set and added into the *Accepted* set. Such a process is the classic find-min operation in computer science, which is considerably time-consuming when the *Trial* set is very large. For better performance, the Fibonacci heap data structure is suggested to store the *Trial* set. The time complexity of find-min operation is $O(1)$ (Cormen, Leiserson, Rivest, & Stein, 2009). For each neighbouring point *a* of **x**, its *u*-values will be updated by using Eq. (5). At the same time, neighbouring points located in the *Far* point set will be moved into the *Trial* point set. The algorithm will end when the *Trial* point set is empty.

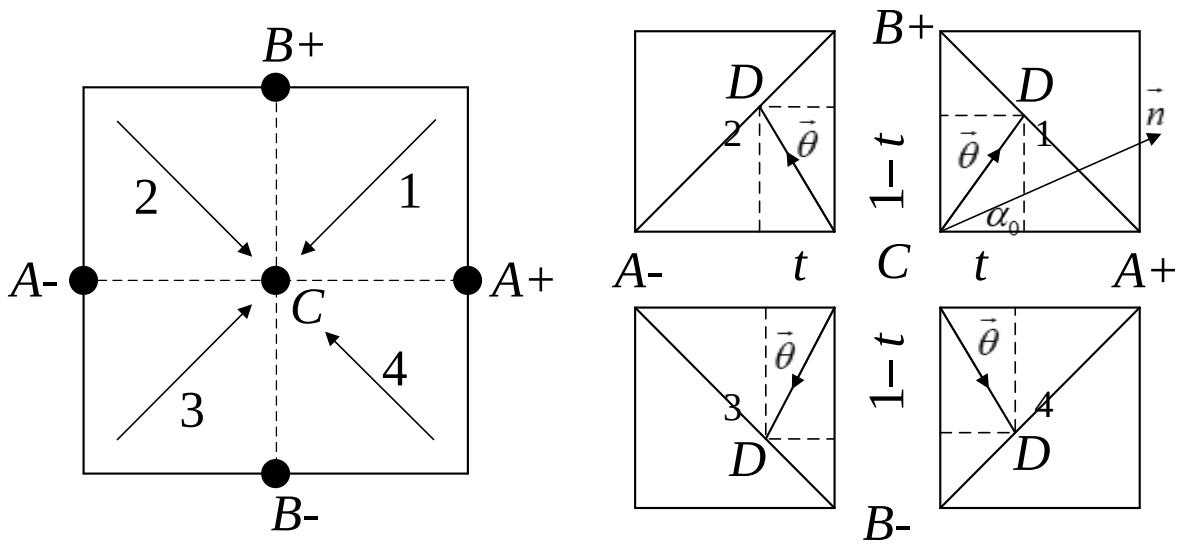

(a) (b)

Fig. 1 The arrival time of point *C* is to be computed from one of the four quadrants around it. (b) The situations in four quadrants.

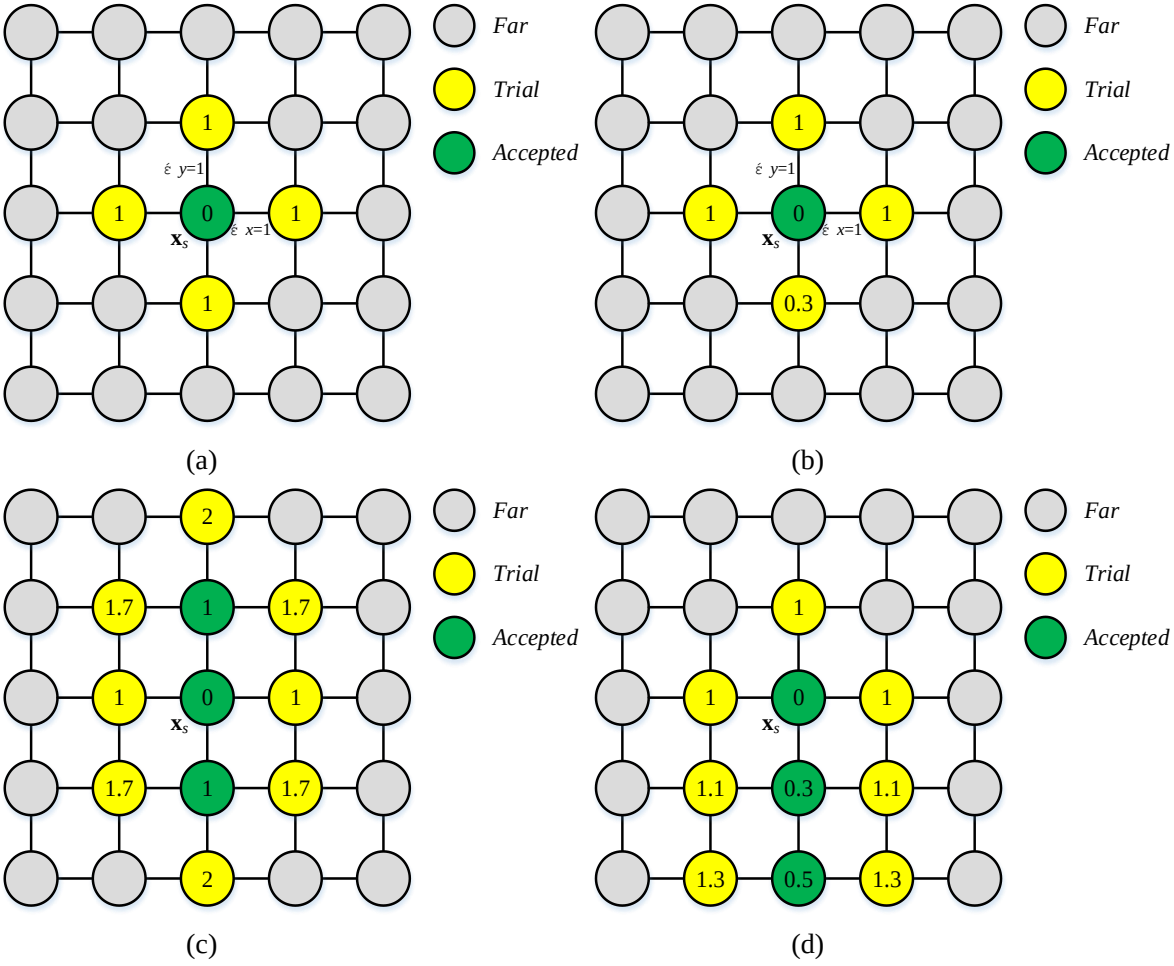

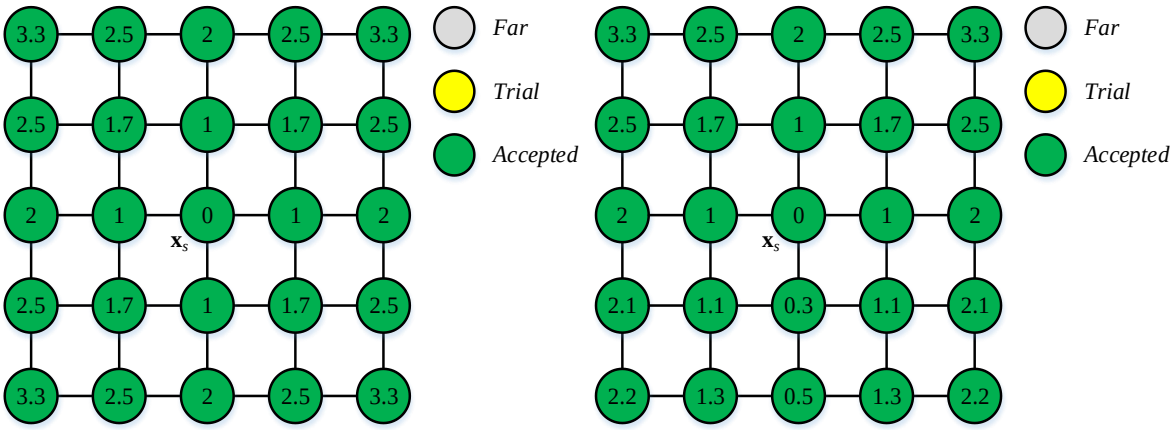

(e) (f)

Fig. 2 The updating process when using the FM method. (a), (c) and (e) are based on the isotropic FM method while (b), (d) and (f) are based on the anisotropic FM method.

Algorithm 1 *Isotropic _FM Algorithm*

Require: configuration space (M), start points ($\mathbf{x}_s$)

Initialise all the grid points in M with the cost of infinity
$U(\mathbf{x}_s) \leftarrow 0$
Far ← All grid points in M
Accepted ← All grid points with known cost
for each neighbouring point a of *Accepted* point **do**
    Trial ← *a* ∪*Trial*
    U(a) ← *Update* by using Eq. (5)
end for
while *Trial* is not empty **do**
    x ← point with the lowest cost in *Trial*
    Remove **x** from *Trial*
    Accepted ← **x** ∪*Accepted*
    for each neighbouring point a of **x do**
        U'(a) ← *Update* by using Eq. (5)
        if U'(a)< U(a) **then**
            U(a) ← U'(a)
        end if
        if a ∈*Far* **then**
            Remove a from *Far*
            Trial ← *a* ∪*Trial*
        end if
    end for
end while

24: **return** U

Algorithm 2 *Anisotropic _FM Algorithm*

Require: configuration space (M), start points ($\mathbf{x}_s$), start points course ($\boldsymbol{\theta}$)

Initialise all the grid points in M with the cost of infinity
$U(\mathbf{x}_s) \leftarrow 0$
$Far \leftarrow$ All grid points in M
$Accepted \leftarrow$ All grid points with known cost
for each neighbouring point a of *Accepted* point p **do**
    $Trial \leftarrow a \cup Trial$
    $\boldsymbol{\theta}(a) \leftarrow \boldsymbol{\theta}(p)$
    $\alpha_0 \leftarrow \boldsymbol{\theta}(a)$
    $U(a) \leftarrow$ *Update* by using Eq. (15) with course α_0
end for
while *Trial* is not empty **do**
    $\mathbf{x} \leftarrow$ point with the lowest cost in *Trial*
    Remove $\mathbf{x}$ from *Trial*
    $Accepted \leftarrow \mathbf{x} \cup Accepted$
    for each neighbouring point a of $\mathbf{x}$ **do**
        $\alpha_0 \leftarrow \boldsymbol{\theta}(\mathbf{x})$
        $U'(a) \leftarrow$ *Update* by using Eq. (15) with course α_0
        if $U'(a) < U(a)$ **then**
            $U(a) \leftarrow U'(a)$
            $\boldsymbol{\theta}(a) \leftarrow \alpha_0$
        end if
        if $a \in Far$ **then**
            Remove a from *Far*
            $Trial \leftarrow a \cup Trial$
        end if
    end for
end while
return U

3.3 The anisotropic fast marching (FM) method

When computing the minimum cumulative cost, the isotropic FM method only uses the location information as input data. It means that the cost function τ is a fixed value at each point. As shown in Eq. (7), τ_C is the cost value at point C. However, when facing a dynamic

obstacle, a fixed value for each point may not be appropriate. By comparison, the anisotropic FM method summarized in Algorithm 2 takes both the location and the local orientation into consideration when executing the marching process (Lin, 2003). Hence, it is more practical in this occasion. The cost functions of the anisotropic FM method, shown as Eq. (8), are defined to be related to both location and orientation.

$$u_C = \min_{t\in[0,1]}\left(tu_{A+} + (1-t)u_{B+} + \left\|\vec{\theta}(t)\right\|\tau_C\left(\vec{\theta}(t)\right)\right). \tag{8}$$

where $\vec{\theta}(t)$ is equal to the vector $\overrightarrow{CD}$ as shown in Fig. 1 and $\tau_C\left(\vec{\theta}(t)\right)$ is called cost function, which is the reciprocal of the speed function. When addressing a particular problem, the speed function needs a specific design.

At any point in the grid map, the cost function depended on location and orientation can be described by a cost/speed profile. In the isotropic case, the speed profile is circular, which is independent of the direction. In the anisotropic case, we chose an oval shape speed profile, which consists of two semi ellipses shown in Fig. 3. Considering the polar coordinate system, the speed profile can be described as (r, α), where α is the local orientation and the r indicates the value of speed. The shape of the speed profile can be adjusted by the three axes of the two semi ellipses. When the three axes are equal to each other, the speed profile becomes the isotropic circular profile. Thus, the anisotropic FM is more general than the isotropic FM. The oval shape speed profile has the following form:

$$\frac{(r\cos\alpha)^2}{\left\{\left(1+\mathrm{sgn}(\cos\alpha)\right)r_a/2+\left(1-\mathrm{sgn}(\cos\alpha)\right)r_b/2\right\}^2}+\frac{(r\sin\alpha)^2}{r_c^{\,2}}=1. \tag{9}$$

where

$$\mathrm{sgn}(\cos\alpha)=\begin{cases}1, & \cos\alpha\ge 0\\ -1, & \cos\alpha<0\end{cases}. \tag{10}$$

α is the intersection angle between $\vec{\theta}(t)$ and $\vec{n}$. The oval shape is aligned with the given direction $\vec{n}$ as shown in Fig. 3.

$$\vec{n}=(\cos\alpha_0,\sin\alpha_0). \tag{11}$$

The vector $\vec{\theta}(t)$ in the four quadrants shown in Fig. 1 is:

$$\vec{\theta}(t)=(\theta_x,\theta_y)=(t,1-t),\ \ (-t,1-t),\ \ (-t,t-1),\ \ (t,t-1). \tag{12}$$

Since the cost and the speed are reciprocal, the cost function $\tau_C\left(\vec{\theta}(t)\right)$ is given as:

$$\tau_C\left(\vec{\theta}(t)\right)=\frac{1}{r}=\sqrt{\frac{\left(\cos\angle\left(\vec{\theta},\,\vec{n}\right)\right)^2}{r_{ab}{}^2}+\frac{\left(\sin\angle\left(\vec{\theta},\,\vec{n}\right)\right)^2}{r_c{}^2}}$$
$$=\frac{1}{\left\|\vec{\theta}\right\|}\sqrt{\frac{\left|\vec{\theta}\square\vec{n}\right|^2}{r_{ab}{}^2}+\frac{\left|\vec{\theta}\times\vec{n}\right|^2}{r_c{}^2}} \quad . \tag{13}$$
$$=\frac{1}{\left\|\vec{\theta}\right\|}\sqrt{\frac{\left(\theta_x\cos\alpha_0+\theta_y\sin\alpha_0\right)^2}{r_{ab}{}^2}+\frac{\left(\theta_x\cos\alpha_0+\theta_y\sin\alpha_0\right)^2}{r_c{}^2}}$$

where

$$r_{ab}=\frac{\left(1+\mathrm{sgn}\left(\theta_x\cos\alpha_0+\theta_y\sin\alpha_0\right)\right)r_a+\left(1-\mathrm{sgn}\left(\theta_x\cos\alpha_0+\theta_y\sin\alpha_0\right)\right)r_b}{2}. \tag{14}$$

The general minimization problem Eq. (8) in this special case is converted into

$$u_C=\min_{t\in[0,1]}\left(tu_{A+}+(1-t)u_{B+}+\sqrt{\frac{\left(\theta_x\cos\alpha_0+\theta_y\sin\alpha_0\right)^2}{r_{ab}{}^2}+\frac{\left(\theta_x\cos\alpha_0+\theta_y\sin\alpha_0\right)^2}{r_c{}^2}}\right). \tag{15}$$

where u_C , u_{A+} and u_{B+} indicate the cumulative travel cost from start point to point *C*, *A*+ and *B*+ respectively as shown in Fig. 1.

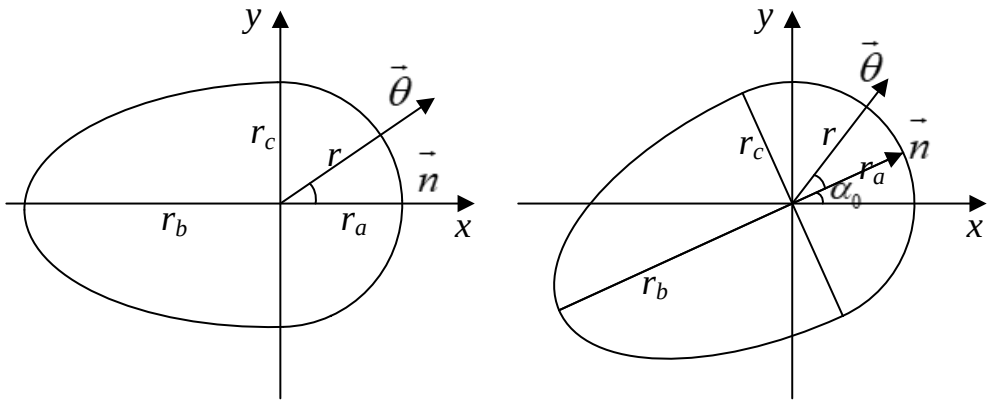

(a) (b)

Fig. 3 (a) An anisotropic oval shape speed profile aligned with the coordinate axis. (b) An oval shape speed profile along the preferred direction $\vec{n}$.

Different expressions can be obtained in different quadrants by substituting Eq. (12) into Eq. (15).

Solving Eq. (15) may also be very difficult. Therefore, an iterative method is proposed to find the minimum value of the cost function. When analysing the cost function, it can be found that its second-order derivative is constantly greater than zero, *i.e*. its first-order derivative is a monotonic function. If the first-order derivative of cost function has a zero value, the bisection

method can be used to obtain it efficiently. Then the minimum value of cost function can directly be obtained. The bisection method is described in Algorithm 3 (Wikipedia, 2018).

Algorithm 3 *Get_ minimum Algorithm*

Input: lower limit (*a*), upper limit (*b*), precision (*e*)

Output: minimum value (u_C)

1: $err \leftarrow \text{abs}(a-b)$
2: **while** (*err*>*e*) **do**
3: **if** $(u_C^{'}(a)*u_C^{'}(b) \geq 0)$
4: **break**
5: **end if**
6: **if** $(u_C^{'}(a)*u_C^{'}((a+b)/2) \geq 0)$
7: $a \leftarrow (a+b)/2$
8: **else**
9: $b \leftarrow (a+b)/2$
10: **end if**
11: $err \leftarrow \text{abs}(a-b)$
12: **end while**
13: **return** $u_C \leftarrow \min(u_C(a), u_C(b))$

3.4 The anisotropic FM-based path planning approach

There are several steps in the FM based path planning approach. The major step is to generate an arrival time map which has a zero value at the start point. Taking the arrival time map as input, the gradient descent method will then be employed to obtain an appropriate and smooth path. Considering that it is difficult to make a turn for a cargo ship and a smooth path is easily tracked, the FM based path planning approach is suitable for ships. Paths with different costs can be generated when using different arrival time maps. Therefore, the key to finding an appropriate path is to find a satisfied arrival time map. Usually, a map of obstacles, generated by target extraction and recognition approaches (Ma, Wu, Yan, Chu, & Zhang, 2015; Ma, Chen, Yan, Chu, & Wang, 2016; Ma, Chen, Yan, Chu, & Wang, 2017), will be used as the input for the path generator and within such a map, the static and dynamic obstacles can be added using a given and unified scale.

Many researchers have studied the FM method and have developed several FM-based path planning approaches. Some of them aim to generate a path by directly using the isotropic FM method. However, it turns out that the generated path is always too close to obstacles in the subsequent applications (Liu & Bucknall, 2016). Such a drawback is especially impractical for smart ships or USVs, since close range areas around obstacles (islands and coastlines) are

usually shallow waters, which are not suitable for navigation. In addition, the danger of being too close to a moving obstacle would also require the planned path to retain a certain distance away from the obstacle.

To tackle this problem, a novel FM based approach named the fast marching square (FMS) was proposed (Gómez, Lumbier, Garrido, & Moreno, 2013). The basic concept behind the FMS is to apply the isotropic FM method twice but with different purposes. As presented in Algorithm 4, the FMS first generates a safety potential map (*Ms*), (also called repulsive force field) by applying the isotropic FM to propagate interfaces from all the points in the obstacle area. Based on the *Ms*, the isotropic FM is executed again from the start point to generate a joint potential field namely the arrival time map mentioned earlier. A gradient descent method is used to produce the final path based on the joint potential field. By using the same previous planning space, the path generated by the FMS is farther away from the obstacles with increased safety.

However, the FMS also has its defects. In the process of path generation, the map of safe area surrounding obstacles is generated by using the isotropic FM method. The planned path is advisable for static obstacles and can meet the requirements for static obstacle avoidance. However, when it occurs to dynamic obstacle avoidance, especially for collision avoidance with ships, the path planned by FMS could not be feasible as they may not be complaint with the dynamic characteristics of ships. Because ships have the feature of incapable of decelerating or accelerating within a short time or making a sharp turning (Liu, Hekkenberg, Quadvlieg, Hopman, & Zhao, 2017), it would become risky for an autonomous ship navigating close to the bow of a ship. Correspondingly, the nearby area in the surrounding ship's stern direction is relatively safe. Also, in practical ship collision avoidance manoeuvres, the give-way vessels normally choose the path passing the stern of the moving ship with a short safe distance. In contrast, when it is required to choose the path passing the bow of the moving ship, a long safe distance is preferred. Therefore, a circular or an eclipse safety area around a dynamic obstacle is not reasonable in the dynamic obstacle avoidance.

To satisfy the requirement of dynamic obstacle avoidance, this paper proposes a novel path planning approach based on the anisotropic FM with significant difference from FMS. When generating the safety potential map, the anisotropic FM-based path planning approach chooses the anisotropic FM instead of the isotropic FM. Considering the characteristics of the safe area around the ship, the oval shape velocity field is used in the anisotropic FM. In this way, when the ship needs to pass the bow of a dynamic obstacle, a path will be generated with a long safe distance to ensure safety. When it is necessary to pass the stern of dynamic obstacle, a path with a relatively short safe distance will be given to balance the cost of safety and distance. Moreover, the proposed approach is capable of describing static obstacles. If the coefficients of anisotropic FM (or the proposed approach) are the same, the anisotropic FM becomes an isotropic FM. In practical path planning, different anisotropic coefficients can be

set under different considerations, such as the obstacle ship's type and speed. The anisotropic FM-based path planning Algorithm is described in Algorithm 5.

Algorithm 4 *Isotropic _FM based path planning Algorithm*

Require: planning space (M), start point ($\mathbf{x}_s$), end point ($\mathbf{x}_e$)

for the *ith* point *a* in obstacle with course θ **do**
    obstaclePoints ←*a* ∪*obstaclePoints*
end for
$\boldsymbol{M}_s$ ←*Isotropic _FM(**M**, obstaclePoints)*
U ←*Isotropic _FM(*$\boldsymbol{M}_s$*,* $\mathbf{x}_s$*)*
path ←*gradientDecent(**U**,* $\mathbf{x}_s$*,* $\mathbf{x}_e$*)*
return *path*

Algorithm 5 *Anisotropic _FM based path planning Algorithm*

Require: planning space (M), start point ($\mathbf{x}_s$), end point ($\mathbf{x}_e$)

for the *ith* point a in obstacle with course θ **do**
    obstaclePoints(i) ←a
    obstaclePointsCourse(i) ← θ
end for
$\boldsymbol{M}_s$ ←*Anisotropic _FM(**M**, obstaclePoints, obstaclePointsCourse)*
U ←*Isotropic _FM(*$\boldsymbol{M}_s$*,* $\mathbf{x}_s$*)*
path ←*gradientDecent(**U**,* $\mathbf{x}_s$*,* $\mathbf{x}_e$*)*
return *path*

4 A case study

In order to validate the performance of the anisotropic FM-based path planning approach, this section builds up a simulation environment to test the approach. Different coefficients of the proposed approach, such as safe distance limitation, oval shape speed profile, crossing angle and number of dynamic obstacles, are assigned for generating the collision free path. By comparing the results of path planning, the relationship between various coefficients and specific environmental factors is established, which can provide a guidance on selecting suitable coefficients for specified practical task.

4.1 Test cases with a single dynamic obstacle

In order to determine the effect of safe distance limitation on path planning, this research sets up different safe distance limitation α values when performing path planning in the same simulation environment. The three coefficients of an oval shape speed profile are set up with a

= 1, b = 0.25, c = 0.25. The course of the obstacle ship is equal to 90°. The path planning result is shown in Fig. 4.

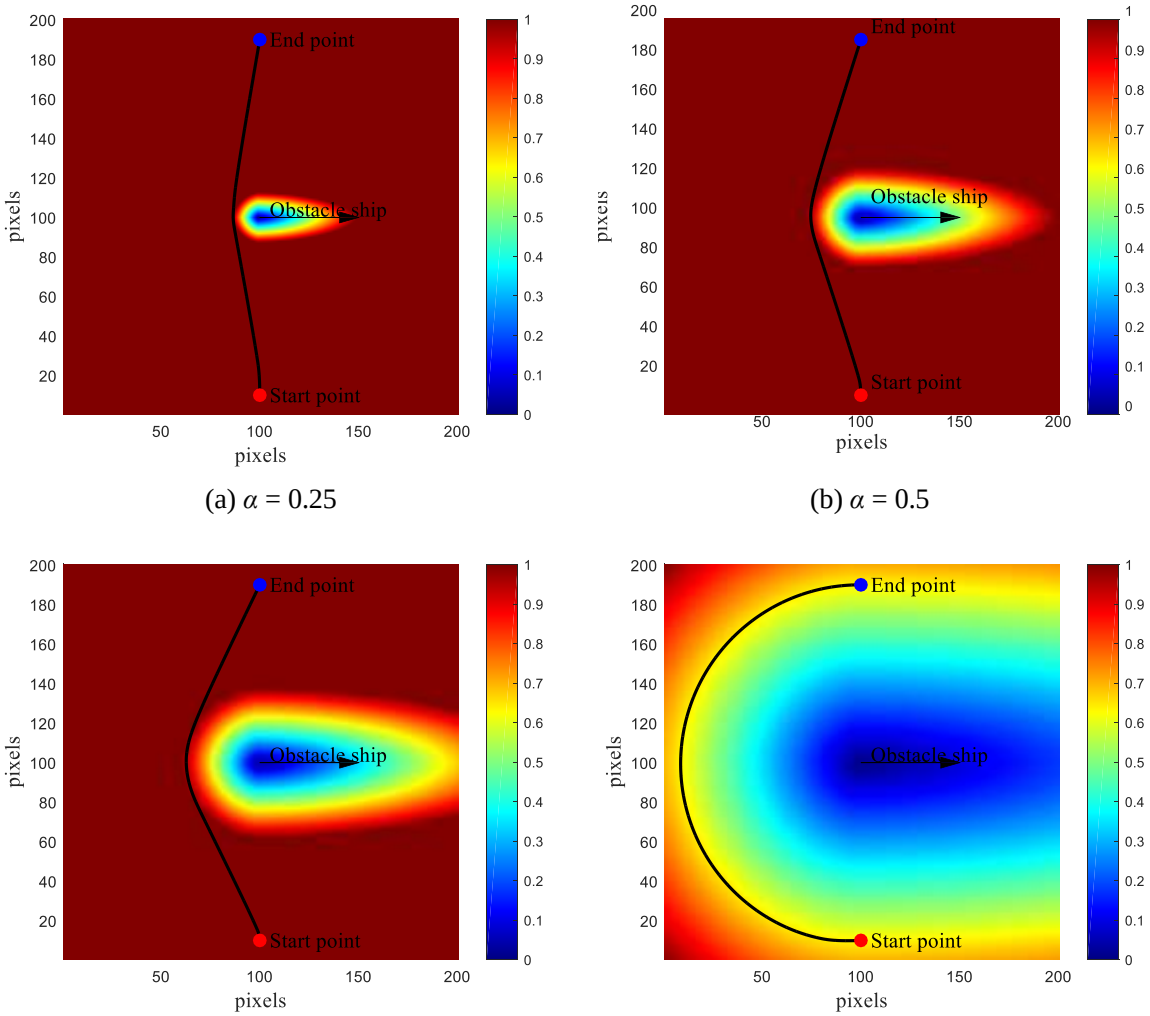

(a) α = 0.25 (b) α = 0.5

(c) α = 0.75 (d) α = 5, 10, …, ∞

Fig. 4 The planning path with different safe distance limit α value, where a = 1, b = 0.25, c = 0.25 and course = 90°.

In order to determine the effect of the oval shape speed profile on path planning, this research sets up a series of simulation experiments with different oval shape speed profile parameters a, b and c. The other coefficients are also given. The safe distance limit α is set as 0.25 and the course of the obstacle ship as 90°. The path planning result is shown in Fig. 5.

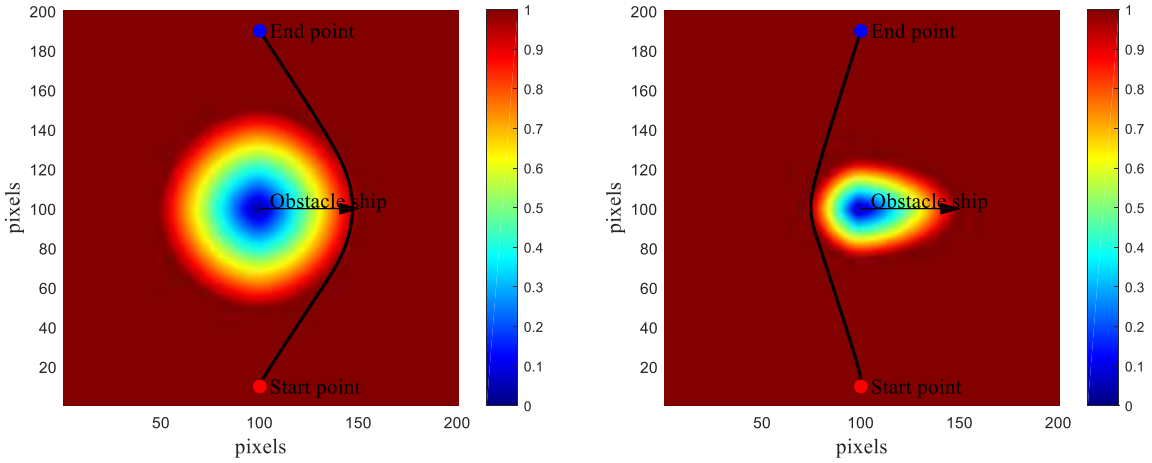

(a) a = 1, b = 1, c = 1

(b) a = 1, b = 0.5, c = 0.5

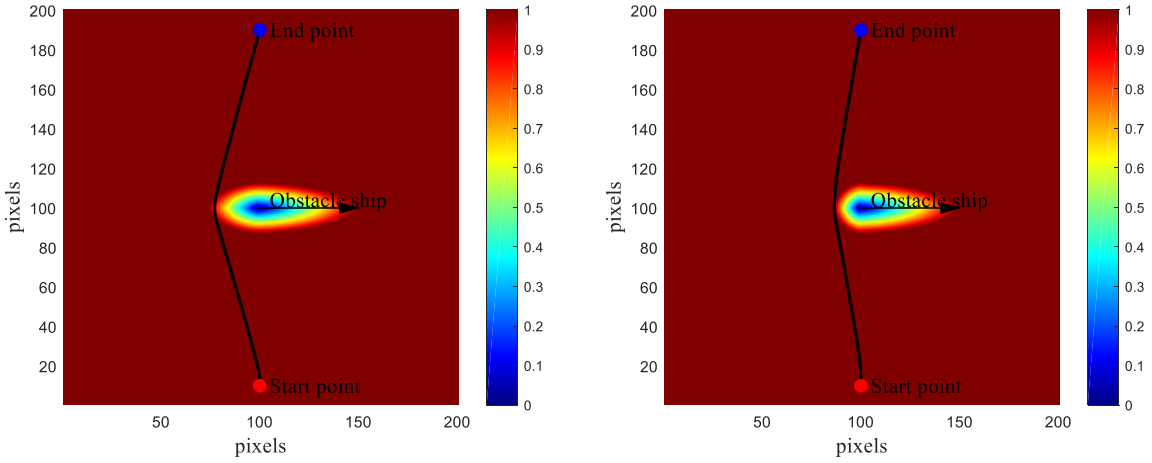

(c) a = 1, b = 0.5, c = 0.25

(d) a = 1, b = 0.25, c = 0.25

Fig. 5 The planning path with different oval shape speed profile, where α = 0.25 and course = 90°.

For further analysis, the path lengths and the minimum distances from the path to the obstacle ship shown in Fig. 4 and Fig. 5 are given in Table 1.

Table 1 The path lengths and the minimum distances from path to the obstacle ship

		Len	D_{min}
Fig. 4	(a)	182.10	12.47
	(b)	187.14	24.34
	(c)	195.27	36.18
	(d)	284.43	89.92
Fig. 5	(a)	205.63	46.73
	(b)	187.66	25.15
	(c)	185.80	22.01
	(d)	182.10	12.47

This study also sets up a series of simulation experiments with different courses of moving ships to evaluate the effect of course on path planning. The other coefficients are set as follow: a = 1, b = 0.25, c = 0.25 and α = 0.25. The path planning result is shown in Fig. 6.

In these tests, it can be seen that a reasonable path can always be generated. When encountering a dynamic obstacle ship, paths can always be generated to keep far away from the bow of the dynamic obstacle ship, meanwhile trying to get pass the stern of the obstacle ship.

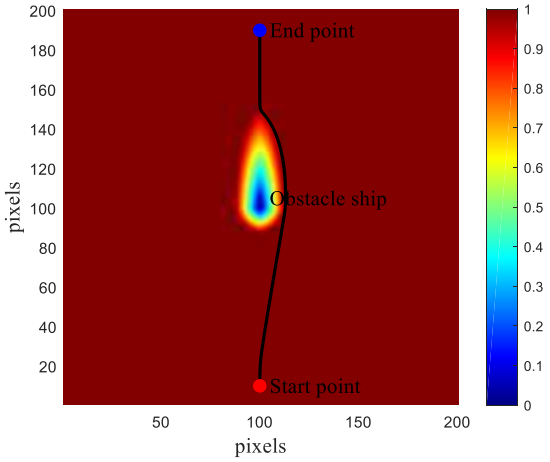

(a) course = 0°

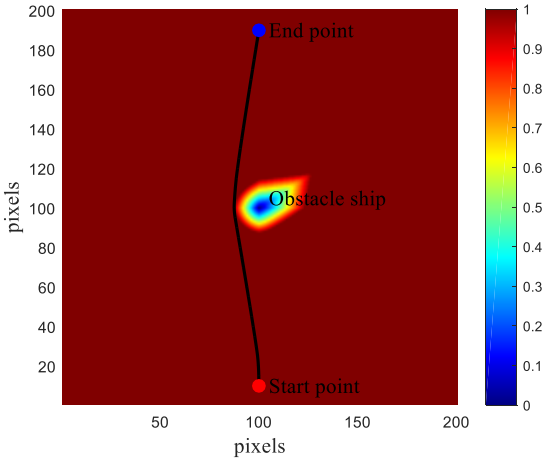

(b) course = 60°

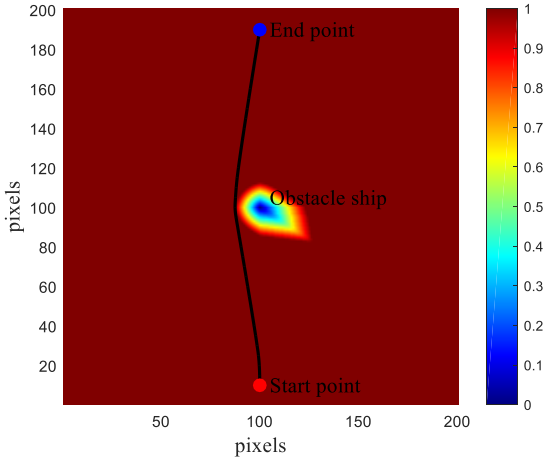

(c) course = 120°

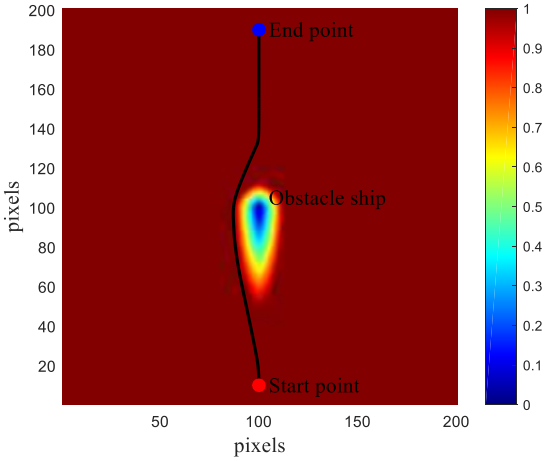

(d) course = 180°

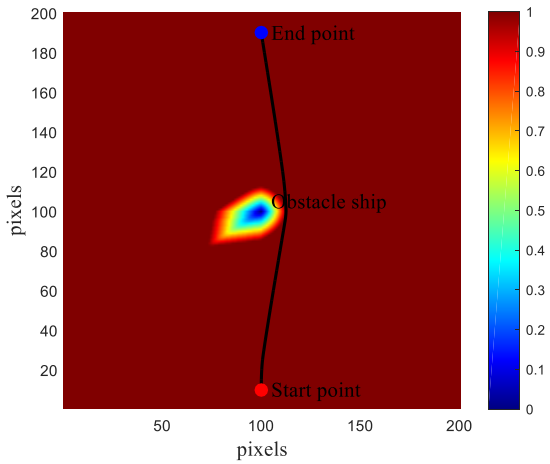

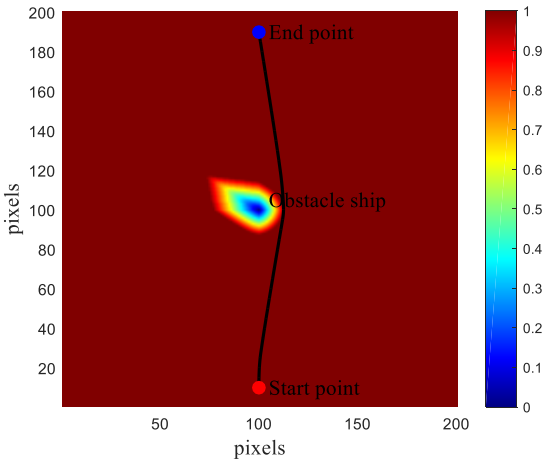

(e) course = 240° (f) course = 300°

Fig. 6 The performance of the anisotropic FM-based path planning approach with different crossing angles, where a = 1, b = 0.25, c = 0.25 and α = 0.25.

4.2 Test cases with multiple dynamic obstacles

To ensure that the proposed path planning approach can be applied to the real environment, it is necessary to test the performance of the approach in more complex environments. This section builds a set of complex dynamic environments, where two dynamic ships and four dynamic ships are involved. The coefficients of simulation environments are set as follow: a = 1, b = 0.25, c = 0.25 and α = 0.25. The path planning result is reasonable as shown in Fig. 7.

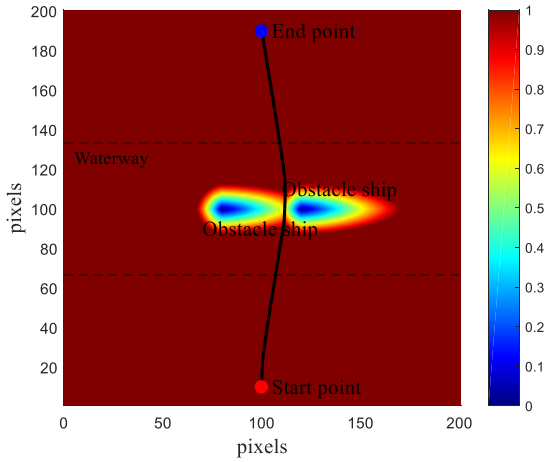

(a) course = 90°

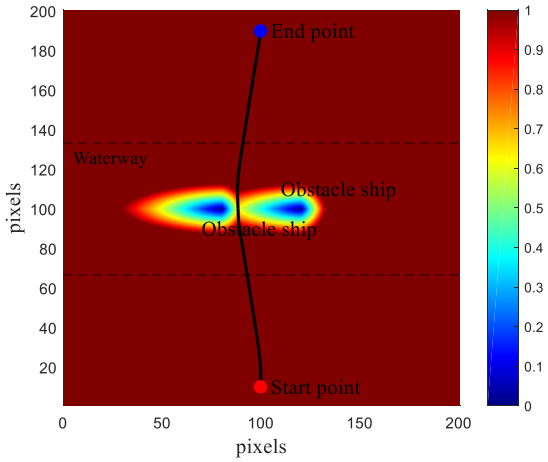

(b) course = 270°

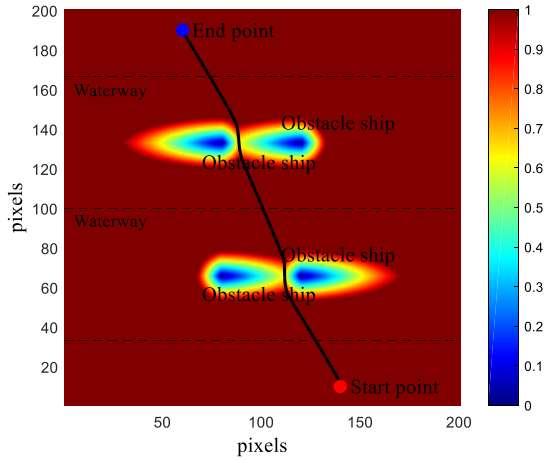

(c) course = 90°, 270°

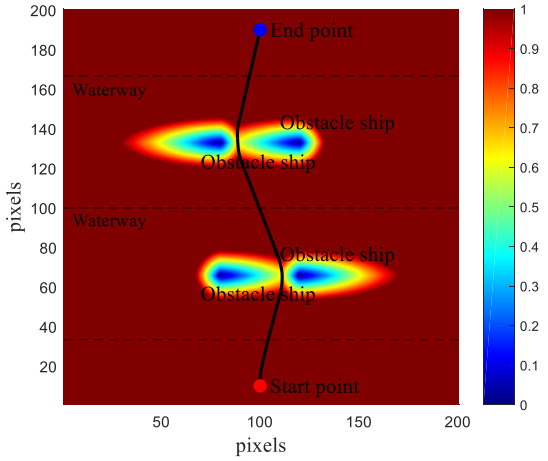

(d) course = 90°, 270°

Fig. 7 The path planning result in complex environments with multiple dynamic obstacles.

In addition, another test is carried out to validate the dynamic performance of the proposed path planning approach. In this test, four dynamic ships are involved and the coefficients of simulation environments are same as the previous test. Besides, speeds of all the obstacle ships are set to 2.0 pixels per time step and the speed of the own ship was equal to 3.5 pixels per time step. During the simulation, the courses of obstacle ship 1 and obstacle ship 2 are 270 degrees

and the courses of obstacle ship 3 and obstacle ship 4 are 90 degrees, respectively. At every time step, the path is updated once and the course of the own ship is changed along the path. The movement sequences of collision avoidance are shown in Fig. 8.

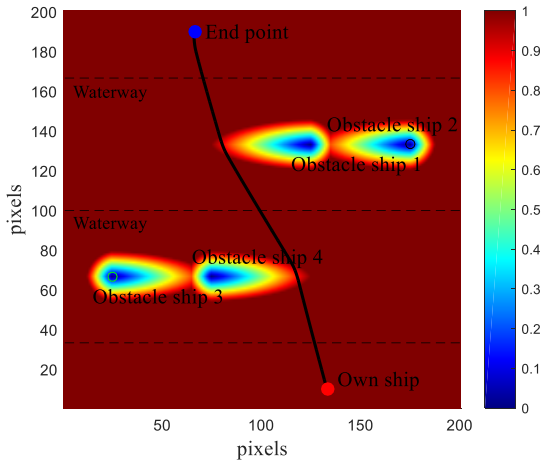

(a) Time step = 1

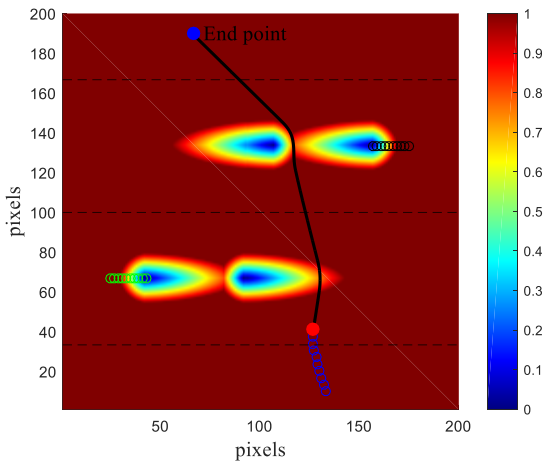

(b) Time step = 10

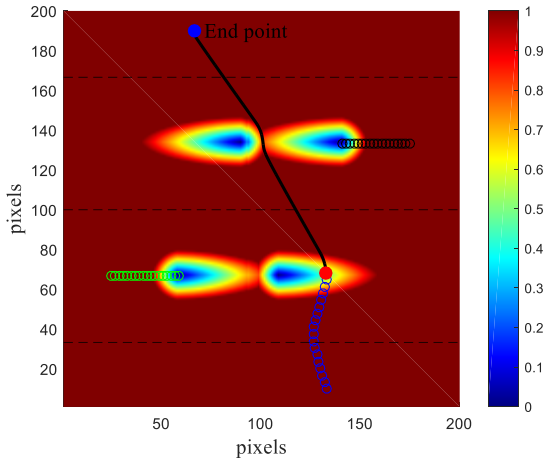

(c) Time step = 17

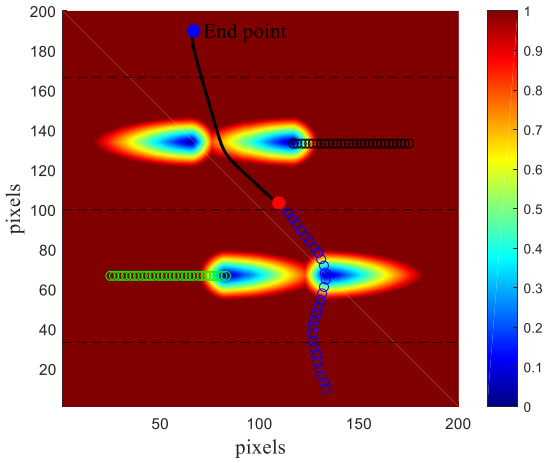

(d) Time step = 30

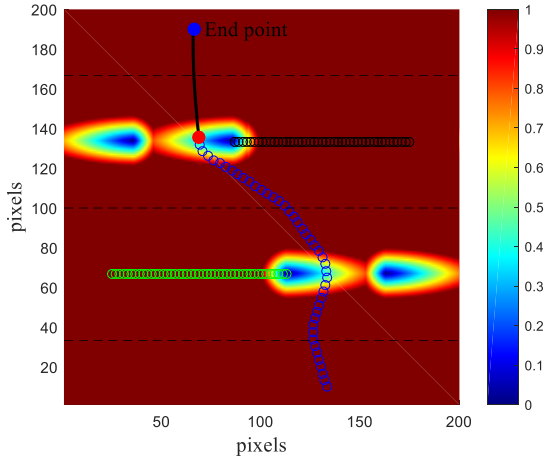

(e) Time step = 45

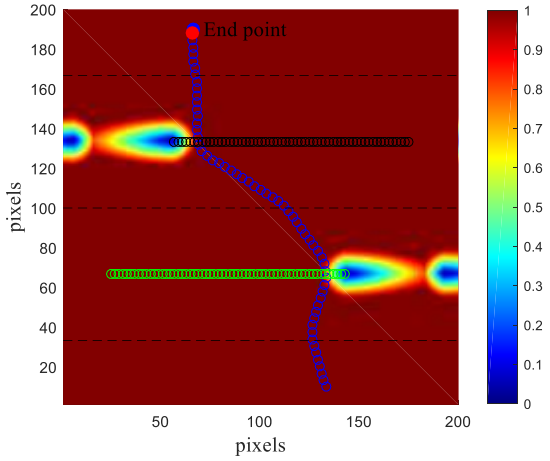

(f) Time step = 60

Fig. 8 The movement sequences of simulation with multiple dynamic obstacles.

4.3 Comparisons with other path planning approaches

For comparisons, the research uses three algorithms, A*, RRT, and RRT* to plan a path in the same environment. The path planning results are shown in Fig. 9. In the simulation, different scenarios have been taken into consideration. As shown in Fig. 9a and Fig. 9b, a simple scenario is used to test these algorithms. Meanwhile, the results in a more complex scenario are shown in Fig. 9c and Fig. 9d. It should be noted that all four algorithms use the same information of the environment. It assumes that the full information including that of obstacle ships is available. In addition, the anisotropic FM method uses the same coefficients used previously in Section 4.2. As shown in Fig. 9, there are four kinds of paths. The black, red, blue and green paths are generated by anisotropic FM, A*, RRT and RRT*, respectively.

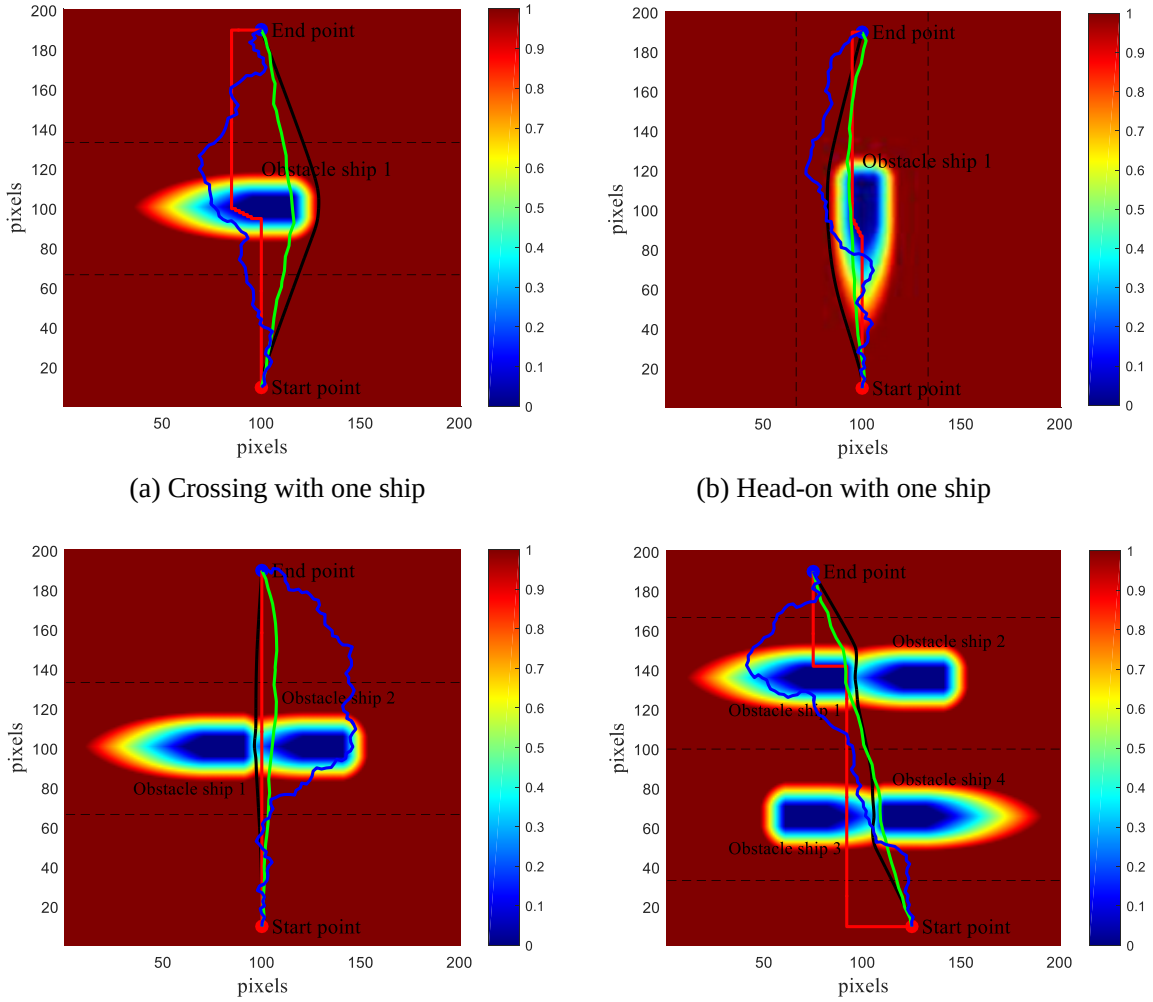

(a) Crossing with one ship

(b) Head-on with one ship

(c) Crossing with two ships

(d) Crossing with multiple ships

Fig. 9 The path planning result with different algorithms (The black, red, blue and green paths are generated by anisotropic FM, A*, RRT and RRT*, respectively.)

In order to quantitatively analyse the performance of the above four path planning approaches, the path length *Len* in pixel is calculated. At the same time, the minimum distance

D_{bowi} and D_{sterni} from the path to the bow and stern of obstacle ship i in pixel are calculated. The results are given in Table 2.

Table 2 The performance indexes of paths generated by the four approaches

		Len	D_{Bow1}	D_{Stern1}	D_{Bow2}	D_{Stern2}	D_{Bow3}	D_{Stern3}	D_{Bow4}	D_{Stern4}
Fig. 9a	FM	190.05	31.96	13.10	\	\	\	\	\	\
	A*	210.00	0.00	15.00	\	\	\	\	\	\
	RRT	240.44	6.08	23.87	\	\	\	\	\	\
	RRT*	184.29	20.22	2.65	\	\	\	\	\	\
Fig. 9b	FM	184.39	12.41	12.27	\	\	\	\	\	\
	A*	190.00	0.00	0.00	\	\	\	\	\	\
	RRT	231.41	7.18	16.15	\	\	\	\	\	\
	RRT*	182.34	1.11	2.57	\	\	\	\	\	\
Fig. 9c	FM	180.26	26.39	6.45	13.55	42.94	\	\	\	\
	A*	180.00	30.00	10.00	10.00	40.00	\	\	\	\
	RRT	273.02	40.33	25.36	8.76	1.27	\	\	\	\
	RRT*	181.72	34.41	14.84	5.72	34.17	\	\	\	\
Fig. 9d	FM	190.84	26.39	6.45	13.54	42.86	15.66	45.15	25.31	4.37
	A*	230.00	5.39	2.00	18.00	48.00	2.00	32.00	39.00	18.00
	RRT	268.85	1.42	14.77	32.75	52.96	11.52	37.86	16.44	4.63
	RRT*	188.67	21.55	1.63	18.01	44.28	19.21	48.37	20.20	1.83

4.4 Result analysis

This section analyses the influences of different coefficients in the anisotropic FM-based path planning approach. One purpose of the test is to elaborate the relationships between the coefficients and factors in path planning. It is possible to figure out how to adjust the coefficients when facing different path planning requirements in practice. Then, the path planning results in a complex environment are fully studied. The performances of anisotropic FM, A*, RRT and RRT* are finally analysed.

As shown in Fig. 4, it can be found that the safe distance limitation α takes a significant influence on planning path. Different α values generate a significant effect on the total length as well as the closest distance to the obstacle ship. When α is set to be 0.25 (Fig. 4a), a very short total length of the planned path is generated and such a generated path is very close to the obstacle ship, with 182.10 pixels and 12.47 pixels respectively. Along with the increase of α (Fig. 4b, Fig. 4c and Fig. 4d), the total length and the closest distance to the obstacle ship of the path generated by the proposed approach increase at the same time as shown in Table 1. When α is large enough, the two features of the generated path discussed previously will reach the maximum value and remain unchanged in the same situation. It is worth noting that a longer length path means a higher distance cost. A farther distance to the obstacle ship means a safer route. In practice, the cost and safety need to be weighed or trade-off when planning a path. If a lower cost is preferred, a smaller α can be considered appropriate. On the contrary, if a farther

distance to the corresponding obstacle ship is needed (e.g. when avoiding like a ship containing hazard chemicals), a larger α is desirable than a smaller one in this occasion.

The coefficients of the oval shape speed profile have a great influence on the safety area map as shown in Fig. 5. When setting these coefficients a, b and c to different values, the shape of the safety area around the obstacle gradually changes from a circular shape (Fig. 5a) to an oval shape (Fig. 5b, Fig. 5c and Fig. 5d). In practice, an obstacle ship with different speeds will be surrounded by different shapes of safe area. A large area in front of a dynamic obstacle and a small area behind can be considered dangerous. It is obvious that when the speed of the dynamic obstacle increases, the area around the bow will become larger and the area behind the stern will decrease at the same time. From Fig. 5, it can be found that, when facing dynamic obstacles, the ratio between a and b can be increased in accordance with the speed of obstacle. When the speed of the obstacle is zero, the radio of the two coefficients will be equal to one, and the anisotropic FM method becomes the isotropic FM. The last coefficient *c* of the oval shape speed profile also has influence on the shape of the safe area. Such a coefficient determines both sides of safe area around a ship. In other words, the coefficient *c* determines the lateral distance between the own ship and obstacles in path planning. It is of great significance in collision avoidance in inland rivers when two waterways are very close to each other.

Fig. 6 presents a series of simulation experiments with different courses of dynamic obstacles in different crossing scenarios. The courses of every two adjacent simulation experiments are changing at the interval of 60 degrees. From Fig. 6, it can be found that the orientation of the safe area is changed by following the course. The anisotropic FM-based path planning approach performs well with different crossing scenarios. No matter what crossing angle is implemented, the proposed approach is capable of planning a safe and satisfied path. However, from this set of simulation experiments, it also can be found that there are some shortcomings in the proposed path planning approach. When the course of the obstacle ship is equal to 0, 90, 180 or 360 degrees, the shape of the safe area is normal. However, when the course of the obstacle ship is equal to other degrees, the shape of the safe area will be slightly deformed. The cause of such a phenomenon is that the anisotropic FM-based approach produces approximate solution when calculating the arrival time to reduce computation as discussed in Section 3.3 and in practice such a shape deformation of the safe area is acceptable (Lin, 2003).

Section 4.2 provides the simulation experiment results of path planning (Fig. 7) using the anisotropic FM-based path planning approach under multiple dynamic obstacles environments. In the simulation, the objective is to generate a short and safe path crossing the waterways, in which ships pass through. In Fig. 7a and Fig. 7b, only one waterway and two ships are considered. The start and end points are on both sides of the waterway. The algorithm should be able to plan the path starting from one side of the waterway to cross the waterway and reach

the other side. The paths generated by the approach are shown in Fig. 7a and Fig. 7b. With a long distance away from the bow of the ship and a short distance away from the stern, the path performs well in the balance or trade-off between the safety and efficiency. When the simulation becomes more complex, which includes two waterways and four obstacle ships, shown in Fig. 7c and Fig. 7d, the path planning approach also performs well. A safe, reasonable and smooth path can always be produced using the proposed approach.

The movement sequences of simulation result with multiple dynamic obstacles are shown in Fig. 8. At the very beginning, an initial path is first generated by the proposed approach and shown in Fig. 8(a) as the black line. The planned path passes through the bow of obstacle ship 1 and 4. At time step 10 (Fig. 8(b)), the own ship re-plans its path to avoid the obstacle ship 4. It is obvious that the own ship prepares to turn right for keeping away from the bow of obstacle ship 4. At time step 17, the own ship safely passes through the bow of obstacle ship 4 as shown in Fig. 8(c). As the own ship proceeds, obstacle ship 1 and obstacle ship 2 start to present a collision threat to the own ship and a new path is planned to avoid the collision. Fig. 8(d)-(f) show how the own ship avoids the obstacle ship 1 and 2 and reaches the end point. The simulation result shows that the proposed approach is capable of safely navigating a ship in a practical situation by adjusting the path at every time step.

In Section 4.3, four algorithms, anisotropic FM, A*, RRT and RRT* are used to plan a path in different scenarios. As shown in Fig. 9 and Table 2, all four algorithms are capable of planning a path without any collision with obstacles. However, it should also be noted that not all paths are suitable for ships to track. For example, the path generated by the A* algorithm is composed of several straight lines and several sharp turns of 90 degrees, which may not be suitable for cargo ships, even if the A* algorithm can sometimes produce a short path as shown in Fig. 9(c). The path produced by the RRT algorithm is not smooth and it is much longer than paths produced by other algorithms making it not an economical option for ships. Compared with the two algorithms, the path planned by RRT* is shorter and smoother. However, all these paths are too close to obstacles, which might be dangerous for cargo ships. Different from these three algorithms, the path produced by the proposed approach in this research is short and safe, and easy to be tracked by a cargo ship.

5 Conclusions

In this paper, a novel path planning approach for smart cargo ships operating in a complex navigation environment, named as anisotropic FM-based approach, has been proposed. Different from the isotropic FM-based path planning approach, the proposed approach uses the anisotropic FM method to obtain a safe map instead of the isotropic FM algorithm. As discussed previously, circular safe areas will be produced for static obstacles and oval shape safe areas will be generated for dynamic obstacles according to their speeds. In other words, different coefficients can be set for the approach to generate reasonably safe areas surrounding both dynamic and static obstacles with any shape according to demands using the same model.

Then, a joint potential field is created to evaluate the travel cost and a reasonable and smooth path can be produced. Although the proposed method shows better performance than A*, RRT and RRT* algorithms, it is also valuable to be compared with other obstacle avoidance methods, including closed-form solutions, for a more complete picture of the advantages and disadvantages of this method. These need to be further studied in the future. The main weakness of the approach is that navigation rules are not considered in the current model.

To improve the approach, a novel decision-making algorithm should be invented in the future to determine the value of safe distance limit (α). As described in Section 4, α is influenced by a number of different factors. For example, when a smart ship is sailing in crowded waters, the value of α will be smaller than the one in normal conditions. By comparison, a larger α might be more appropriate when it occurs to a large ship sailing in the ocean. Research to determine the safe distance limit is of great significance to make use of the human knowledge of avoiding collision with the encounter obstacles. In practical applications, different coefficients should be given in response to different obstacles (e.g. reefs, container ships and chemical carriers). Based on sufficient samples collected by radar or Automatic Identification System (AIS), such coefficients should be obtained by machine learning algorithms.

The second improvement is to optimize the coefficients of oval shape speed profiles in practical environmental constraints. As discussed previously, an oval shape speed profile is specifically designed for dynamic obstacles when producing a safe area map. The key distinction between dynamic and static obstacles is the speed. Hence, it is necessary to consider the moving speed of obstacles when determining such coefficients in practical. If an obstacle moves with a high speed, a long safe distance will be required when passing through the bow of such an obstacle. On the contrary, a short safe distance will be required when passing through the stern of the obstacle. Such research can improve the knowledge of inherent relation between the speed and surrounding safe area of obstacles. In practice, the historical data from ferries can be used to train the coefficients of the oval shape speed profile.

The third improvement is to take the navigation rules into consideration. In particular, evasive actions should be generated by adhering to the maritime navigation regulations (COLREGs). Therefore, a reasoning model is required for the agent to obey the COLREGs. This kind of research contributes to build rule-based intelligent systems. It is important to note that ships navigating in different waters may need to obey specific rules.

Acknowledgements

This work is financially supported by the National Natural Science Foundation of China under Grant No. 61503289, and the Double First-rate Project of WUT under Grant No. 472-20163042. This research is also partially supported by EU H2020 RISE 2016 RESET – 730888.

References

Adalsteinsson, D., & Sethian, J. A. (1995). A fast level set method for propagating interfaces. *Journal of computational physics, 118*(2), 269-277.

Antão, P., & Soares, C. G. (2008). Causal factors in accidents of high-speed craft and conventional ocean-going vessels. *Reliability Engineering & System Safety, 93*(9), 1292-1304.

Abu-Tair, M., & Naeem, W. (2012, September). A decision support framework for collision avoidance of unmanned maritime vehicles. In *International Conference on Intelligent Computing for Sustainable Energy and Environment* (pp. 549-557). Springer, Berlin, Heidelberg.

Alvarez, D., Gómez, J. V., Garrido, S., & Moreno, L. (2015, June). Geometrically constrained path planning with Fast Marching Square. In *Control and Automation (MED), 2015 23th Mediterranean Conference on* (pp. 1014-1019). IEEE.

Crandall, M. G., & Lions, P. L. (1983). Viscosity solutions of Hamilton-Jacobi equations. *Transactions of the American mathematical society, 277*(1), 1-42.

Cohen, L. D., & Deschamps, T. (2001, September). Multiple contour finding and perceptual grouping as a set of energy minimizing paths. In *International Workshop on Energy Minimization Methods in Computer Vision and Pattern Recognition* (pp. 560-575). Springer, Berlin, Heidelberg.

Cormen, T. H., Leiserson, C. E., Rivest, R. L., & Stein, C. (2009). Introduction to algorithms (third edition). *MIT press* (Chapter 20).

Celik, M., & Cebi, S. (2009). Analytical HFACS for investigating human errors in shipping accidents. *Accident Analysis & Prevention, 41*(1), 66-75.

Chen, L. J., Yan, X. P., Huang, L. W., Yang, Z. L., & Wang, J. (2018). A systematic simulation methodology for LNG ship operations in port waters: a case study in Meizhou Bay. *Journal of Marine Engineering & Technology, 17*(1), 12-32.

Dijkstra, E. W. (1959). A note on two problems in connexion with graphs. *Numerische mathematik, 1*(1), 269-271.

Garrido, S., Moreno, L., & Blanco, D. (2008). Exploration of a cluttered environment using Voronoi Transform and Fast Marching. *Robotics and Autonomous Systems, 56*(12), 1069-1081.

Garrido, S., Moreno, L., & Lima, P. U. (2011). Robot formation motion planning using fast marching. *Robotics & Autonomous Systems, 59*(9), 675-683.

Garrido, S., Malfaz, M., & Blanco, D. (2013). Application of the fast marching method for outdoor motion planning in robotics. *Robotics & Autonomous Systems, 61*(2), 106-114.

Gómez, J. V., Lumbier, A., Garrido, S., & Moreno, L. (2013). Planning robot formations with fast marching square including uncertainty conditions. *Robotics and Autonomous Systems, 61*(2), 137-152.

Hidalgo-Paniagua, A., Bandera, J. P., Ruiz-de-Quintanilla, M., & Bandera, A. (2018). Quad-RRT: A real-time GPU-based global path planner in large-scale real environments. *Expert Systems with Applications, 99*, 141-154.

Jaillet, L., Cortés, J., & Siméon, T. (2008, September). Transition-based RRT for path planning in continuous cost spaces. In *Intelligent Robots and Systems, 2008. IROS 2008. IEEE/RSJ International Conference on* (pp. 2145-2150). IEEE.

Kavraki, L., Svestka, P., Latombe, J., & Overmars, M. (1994). Probabilistic roadmaps for path planning in high-dimensional configuration spaces. *IEEE Trans on Robotics & Automation, 12*(4), 566-580.

Kala, R. (2012). Multi-robot path planning using co-evolutionary genetic programming. *Expert Systems with Applications, 39*(3), 3817-3831.

Lin, Q. (2003). *Enhancement, extraction, and visualization of 3D volume data* (Doctoral dissertation, Linköping University Electronic Press).

Liu, Y., & Bucknall, R. (2015). Path planning algorithm for unmanned surface vehicle formations in a practical maritime environment. *Ocean Engineering, 97*, 126-144.

Liu, Y., & Bucknall, R. (2016). The angle guidance path planning algorithms for unmanned surface vehicle formations by using the fast marching method. *Applied Ocean Research, 59*, 327-344.

Liu, J., Hekkenberg, R., Quadvlieg, F., Hopman, H., & Zhao, B. (2017). An integrated empirical manoeuvring model for inland vessels. *Ocean Engineering, 137*, 287-308.

Liu, Y., Bucknall, R., & Zhang, X. (2017). The fast marching method based intelligent navigation of an unmanned surface vehicle. *Ocean Engineering, 142*, 363-376.

Mitchell, J. S., & Papadimitriou, C. H. (1991). The weighted region problem: finding shortest paths through a weighted planar subdivision. *Journal of the ACM (JACM), 38*(1), 18-73.

Mitchell, J. S. (2000). Geometric shortest paths and network optimization. *Handbook of computational geometry, 334*, 633-702.

Montiel, O., Orozco-Rosas, U., & Sepúlveda, R. (2015). Path planning for mobile robots using Bacterial Potential Field for avoiding static and dynamic obstacles. *Expert Systems with Applications, 42*(12), 5177-5191.

Ma, F., Wu, Q., Yan, X., Chu, X., & Zhang, D. (2015). Classification of automatic radar plotting aid targets based on improved fuzzy C-means. *Transportation research part c: emerging technologies, 51*, 180-195.

Ma, F., Chen, Y. W., Yan, X. P., Chu, X. M., & Wang, J. (2016). A novel marine radar targets extraction approach based on sequential images and Bayesian Network. *Ocean Engineering, 120*, 64-77.

Ma, F., Chen, Y. W., Huang, Z. C., Yan, X. P., & Wang, J. (2016). A novel approach of collision assessment for coastal radar surveillance. *Reliability Engineering & System Safety, 155*, 179-195.

Ma, F., Chen, Y. W., Yan, X. P., Chu, X. M., & Wang, J. (2017). Target recognition for coastal surveillance based on radar images and generalised Bayesian inference. *IET Intelligent Transport Systems, 12*(2), 103-112.

Petres, C., Pailhas, Y., Patron, P., Petillot, Y., Evans, J., & Lane, D. (2008). Path planning for autonomous underwater vehicles. *IEEE Transactions on Robotics, 23*(2), 331-341.

Rouy, E., & Tourin, A. (1992). A viscosity solutions approach to shape-from-shading. *SIAM Journal on Numerical Analysis, 29*(3), 867-884.

Rolls-Royce. Autonomous ship-The next step [EB/OL]. (2016). http://www.rolls-royce.com/~/media/Files/R/Rolls-Royce/documents/customers/marine/ship-intel/rr-ship-intel-aawa-8pg.pdf. Accessed 3 September 2016.

Spahn, J., Dorp, R. V., & Merrick, J. (1998). Using system simulation to model the impact of human error in a maritime system. *Safety Science, 30*(1), 235-247.

Smierzchalski, R. (1999). Evolutionary trajectory planning of ships in navigation traffic areas. *Journal of Marine Science & Technology, 4*(1), 1-6.

Tsitsiklis, J. N. (1995). Efficient algorithms for globally optimal trajectories. *IEEE Transactions on Automatic Control, 40*(9), 1528-1538.

Tam, C. K., & Bucknall, R. (2010). Path-planning algorithm for ships in close-range encounters. *Journal of Marine Science & Technology, 15*(4), 395-407.

Tsou, M. C., & Hsueh, C. K. (2010). The study of ship collision avoidance route planning by ant colony algorithm. *Journal of Marine Science & Technology, 18*(5), 746-756.

Tam, C. K., & Bucknall, R. (2013). Cooperative path planning algorithm for marine surface vessels. *Ocean Engineering, 57*(2), 25-33.

Wikipedia. Bisection method (2018). https://en.wikipedia.org/wiki/Bisection_method. Accessed 25 November 2018.

Xue, Y., Clelland, D., Lee, B. S., & Han, D. (2011). Automatic simulation of ship navigation. *Ocean Engineering, 38*(17–18), 2290-2305.

Yan, X. P., Wu, C., Ma, F. (2017). Conceptual design of navigation brain system for intelligent cargo ship. *Navigation of China,* (4), 95-98.